# APPENDIX A
# DIFFERENCES IN GENERALIZATION COMPARED TO RELATED WORKS

We summarize the distinctions between our approach and existing works. Many studies [1]–[6] are limited to problems that optimize for a single preference. Li te al. [3] employ a Q-learning-based deep reinforcement learning (DRL) method to solve the computation offloading problem in a multi-user environment. Cui et al. [1] decomposes user association, offloading decision, computing, and communication resource allocation into two related sub-problems and employs the DQN algorithm for decision-making. Lei et al. [2] proposed a DRL-based joint computation offloading and multi-user scheduling algorithm for IoT edge computing systems, aiming to minimize the long-term weighted sum of delay and power consumption under stochastic traffic arrivals. Huang et al. [4] employed an improved DQN method to address offloading decision problems and resource allocation problems. The above works focus on two objectives, delay and energy consumption, and use a weight coefficient to balance them or optimize one objective while satisfying the constraints of the other. Moreover, these studies lack research on the generalization.

Some studies [7]–[11] focus only on the generalization of system parameters. Li et al. [7] combine graph neural networks and seq2seq networks to make decisions on task offloading. They employ a meta-reinforcement learning approach to enhance the generalization of the offloading strategy in environments with different system parameters. Ren et al. [8] design a set of experience maintaining and sampling strategies to improve the training process of DRL, enhancing the model's generalization to different environments. Wang et al. [9] design an offloading decision algorithm based on meta-reinforcement learning, which uses a seq2seq neural network to represent the offloading policy. This approach can adapt to various environments covering a wide range of topologies, task numbers, and transmission rates. Wu et al. [10] propose a method that combines graph neural networks and DRL, which can be applied to various environments with inter-dependencies among different tasks. Hu et al. [11] propose a size-adaptive offloading scheme and a setting-adaptive offloading component, designed to quickly adapt to new MEC environments of varying sizes and configurations with a few interaction steps. The above work only considers generalization in terms of system parameters, without addressing generalization in terms of the number of servers and multi-preference issues.

Other works [12]–[14] only consider the generalization of the number of servers. A few works consider the generalization of both system parameters and the number of servers. Gao et al. [15] model the decentralized task offloading problem as a partially observable Markov decision process and use a multi-agent RL method to train the policy. They consider the generalization of both system parameters and the number of servers, but do not explore multi-preference issues. Our method provides a deeper exploration of the generalization of the offloading strategy, considering the generalization in terms of multi-preference, system parameters, and server quantities.

# APPENDIX B
# SUPPLEMENTARY FIGURES

## *B.1 System Model*

The MEC system model we consider is illustrated in Fig. A1. An MEC system consists of $E$ edge servers, one remote cloud server. The system processes $M$ tasks arriving sequentially, with each task being uploaded to only one server.

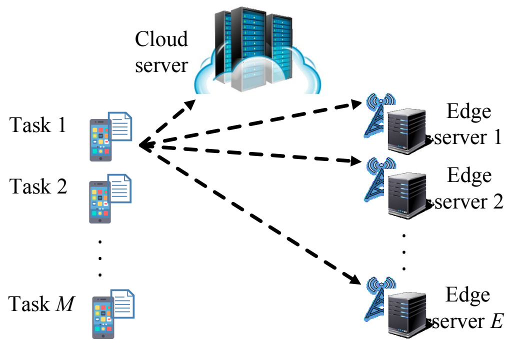


Fig. A1: An illustrative example system model of MEC.

## *B.2 Learning Approach*

During the training phase, we sample $N_{\mathrm{g}}$ contexts to create $N_{\mathrm{g}}$ MEC environments for each epoch. The preferences of these environments are determined by Eq. (32), while their number of servers $E$ and frequencies $\boldsymbol{f}_{\mathcal{E}}$ are randomly drawn from the context space. These environments interact with the policy to generate experiences, which are stored in the replay buffer and used to update the policy.

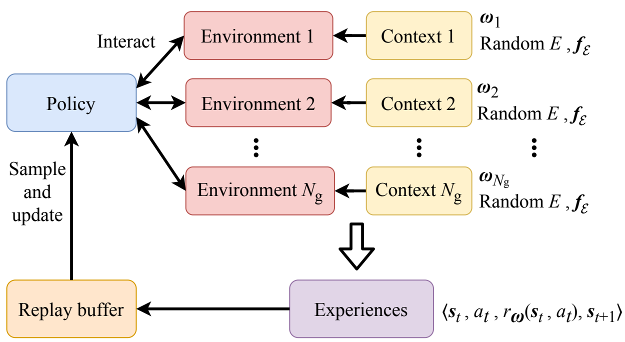


Fig. A2: The generalization learning approach.

## *B.3*

The structure of the GMORL algorithm is illustrated in Fig. A3.

TABLE A1
CONTEXT SPACE FOR TRAINING AND TESTING

| **Context space** | **Training** | **Testing** |
|---|---|---|
| The number of preference $N_g$ | 64 | 101 |
| Edge server quantity $\mathcal{C}_E$ | $\{1, 2, \ldots, 8\}$ | $\{1, 2, \ldots, 10\}$ |
| Cloud server CPU frequency $\mathcal{C}_{f_0}$ | $[3.5, 4.5]$ GHz | $[3.0, 5.0]$ GHz |
| Edge server CPU frequency $\mathcal{C}_{\boldsymbol{f}_{\mathcal{E}'}}$ | $[1.75, 2.25]$ GHz | $[1.5, 2.5]$ GHz |

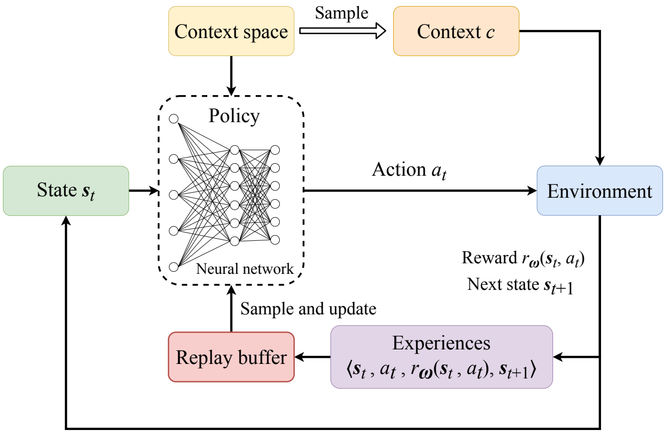


Fig. A3: The overview of the GMORL algorithm.

# APPENDIX C
# SIMULATION SETUP

We provide the context in Table A1. We set testing preference set $\Omega_{N_g}$ according to Eq. (32) and fit Pareto front in $N_g$ preferences. Each preference's performance contains total delay and energy consumption for all tasks in one episode. We evaluate a performance (delay or energy consumption) with an average of 1000 episodes. A disk coverage has a radius of 1000m to 2000m for a cloud server and 50m to 500m for an edge server. Each episode needs to initial different radiuses for the cloud and edge servers. We set the mean of task size $\bar{L}$ according to Eq. (1).

## *C.1 Evaluation Metrics*

We consider the following metrics to evaluate the performances of the proposed algorithms.

- **Energy Consumption:** The total energy consumption of one episode given as $\sum_{m=1}^{M} E_m^{\text{off}} + E_m^{\text{exe}}$, and the average energy consumption per Mbits task of one episode given by $\sum_{m=1}^{M} \frac{E_m^{\text{off}} + E_m^{\text{exe}}}{\bar{L}}$.
- **Task Delay:** The total energy consumption of one episode given as $\sum_{m=1}^{M} E_m^{\text{off}} + E_m^{\text{exe}}$, and the average energy consumption per Mbits task of one episode given by $\sum_{m=1}^{M} \frac{E_m^{\text{off}} + E_m^{\text{exe}}}{\bar{L}}$.
- **Pareto Front:** $PF(\Pi) = \{\pi \in \Pi \mid \nexists \pi' \in \Pi : \boldsymbol{y}^{\pi'} \succ_P \boldsymbol{y}^{\pi}\}$, where the symbols are defined by Eq. (12).
- **Hypervolume Metric:** $\mathcal{V}(PF(\Pi)) = \int_{\mathbb{R}^2} \mathbb{I}_{V_h(PF(\Pi))}(z)dz$, where the symbols are defined by Eq. (14).

## *C.2 Baselines*

*LinUCB-based scheme*: The Offloading scheme is based on a kind of contextual MAB algorithm [16]. It is an improvement over the traditional UCB algorithm. This scheme uses states as MAB contexts and learns a policy by exploring different actions. We apply the multi-arm bandit algorithm. We regard each action as an arm and construct the feature of an arm from preference $\boldsymbol{\omega}$ and server information vector $\boldsymbol{s}_{t,e}$. Then, we update the parameter matrix based on the context and exploration results to learn a strategy that maximizes rewards. We train this scheme in preference set $\Omega_{101}$ and evaluate it for any preference in one. This method is computationally simple and incorporates context information, making it widely used in task offloading.

*SA-based scheme*: The heuristic method searches for an optimal local solution for task offloading without contexts. We use this method to observe the performance of heuristic approaches. This method generates a fixed offloading scheme for each preference and then iteratively searches for better solutions through local search. Once a better solution is found, it is accepted or rejected with a certain probability. This scheme searches 10000 episodes for each preference. However, searching for a solution that only applies to a specific context is time-consuming.

*Random-based scheme*: The random-based scheme has $p$ probability to offload a task to the cloud server and $1-p$ probability to a random edge server. We tune the probability $p$ and evaluate the scheme to obtain a Pareto front.

*Multi-policy scheme*: The multi-policy MORL approach [13] is based on the standard Discrete-SAC algorithm. We build 101 Discrete-SAC policy models for the 101 preference in $\Omega_{101}$ correspondingly. We train each policy model with $f_0 = 4$ GHz and $f_{e'} = 2$ GHz. This method has no generalization ability. A well-trained policy model is applicable to a specific context. However, benefiting from focusing on a specific context, this method is more likely to achieve optimal performance. We apply the method to determine the upper bound of the Pareto front.

## *C.3 Convergence Performances*

We verify the convergence of the proposed GMORL algorithm. In Fig. A4a, we evaluate and plot the training reward of our algorithm. The reward shown in this figure is scalarized using Eq. (29). We observe that with the training episode increasing, the total reward converges. In fig. A4b and fig. A4c, as the training episodes increase, the delay and energy consumption decrease and converge to a stable value. This indicates that the GMORL algorithm converges effectively and reach a Pareto local optimum. In the following subsection, we will specifically analyze other performances in various system settings.

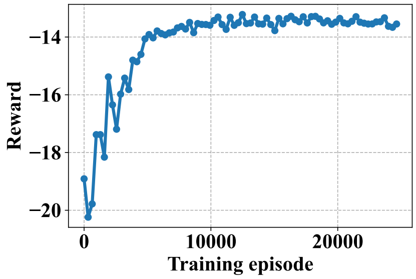


(a)

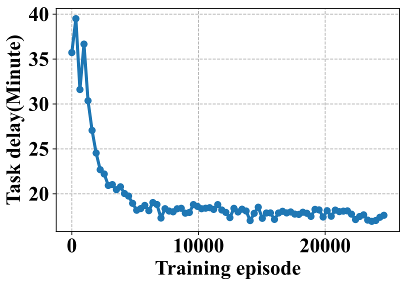


(b)

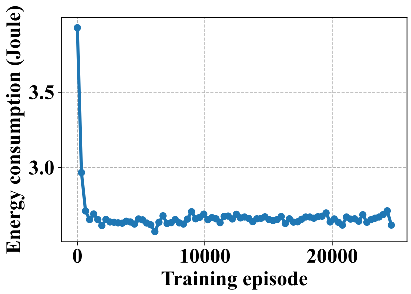


(c)

Fig. A4: Convergence performance of the proposed GMORL algorithm: (a) Reward during training; (b) Total delay during training when $E = 5$, $f_0 = 4$ GHz, $f_{e'} = 2$ GHz for all $e' \in \mathcal{E}'$, and $\boldsymbol{\omega} = (1, 0)$; (c) Total energy consumption during training when $E = 5$, CPU frequency $f_0 = 4$ GHz, $f_{e'} = 2$ GHz for all $e' \in \mathcal{E}'$, and preference $\boldsymbol{\omega} = (0, 1)$.

## Appendix D
## Proof of Theorems

### D.1 Proof of Theorem 1

*Proof.* To prove the convergence of the GMORL algorithm, we analyze the algorithm with the scalarized reward structure. The Bellman operator $\mathcal{T}$ of the action-value function with the scalarized reward is:

$$\mathcal{T}^{\pi} Q(\boldsymbol{s}_t, a_t) = r_{\boldsymbol{\omega}}(\boldsymbol{s}_t, a_t) + \gamma \mathbb{E}_{\boldsymbol{s}_{t+1} \sim \rho_{\pi}}(V(\boldsymbol{s}_{t+1})), \quad \text{(A1)}$$

where $r_{\boldsymbol{\omega}}(\boldsymbol{s}_t, a_t) = \boldsymbol{\omega}^T \times (\alpha_{\mathrm{T}} r_{\mathrm{T}}(\boldsymbol{s}_t, a_t), \alpha_{\mathrm{E}} r_{\mathrm{E}}(\boldsymbol{s}_t, a_t))$ is a scalarized reward function.

For any two policies $\pi$ and $\pi'$, the difference of the Bellman operators is:

$$\begin{aligned}
\|\mathcal{T}^{\pi} Q - \mathcal{T}^{\pi'} Q'\| &= \max_{\boldsymbol{s}} \left| \mathcal{T}^{\pi} Q(\boldsymbol{s}, a) - \mathcal{T}^{\pi'} Q'(\boldsymbol{s}, a) \right| \\
&= \max_{\boldsymbol{s}} \Big| r_{\boldsymbol{\omega}}(\boldsymbol{s}, a) + \gamma \mathbb{E}_{\boldsymbol{s}_{t+1} \sim \rho_{\pi}}(V(\boldsymbol{s}_{t+1})) \\
&\quad - \left( r_{\boldsymbol{\omega}}(\boldsymbol{s}, a) + \gamma \mathbb{E}_{\boldsymbol{s}_{t+1} \sim \rho_{\pi'}}(V'(\boldsymbol{s}_{t+1})) \right) \Big| \\
&= \max_{\boldsymbol{s}} \left| \gamma \mathbb{E}_{\boldsymbol{s}_{t+1} \sim \rho_{\pi}} (V(\boldsymbol{s}_{t+1}) - V'(\boldsymbol{s}_{t+1})) \right| \\
&\leq \gamma \max_{\boldsymbol{s}} |V(\boldsymbol{s}_{t+1}) - V'(\boldsymbol{s}_{t+1})| \\
&\leq \gamma \|Q - Q'\|,
\end{aligned} \quad \text{(A2)}$$

Since $\mathcal{T}$ remains a contraction mapping even with the scalarized reward (as $\boldsymbol{\omega}$ and $\alpha$ coefficients are fixed and do not affect the contraction property), the Banach fixed-point theorem guarantees the existence of a unique fixed point $Q^*$ such that:

$$Q^* = \mathcal{T} Q^*. \quad \text{(A3)}$$

Thus, we have:

$$\lim_{k \to \infty} Q_k = Q^*, \quad \text{(A4)}$$

where $Q_{k+1} = \mathcal{T} Q_k$.

Next, we analyze the convergence of the policy network and the target networks. As the Q-functions converge towards $Q^*$, the policy network updates drive the policy $\pi_{\boldsymbol{\phi}}$ towards the optimal policy $\pi^*$ that maximizes these Q-values. The target networks use the soft update rule: $\bar{\boldsymbol{\theta}}_i \leftarrow \beta \boldsymbol{\theta}_i + (1-\beta) \bar{\boldsymbol{\theta}}_i$, where $\beta \in (0, 1)$ to reduce the risk of divergence caused by changing Q-value estimates. Therefore, we prove the convergence properties of GMORL.

### D.2 Proof of Corollary 1

*Proof.* The computational complexity of this algorithm can be assessed using several parameters. During environment sampling, relevant context and features are generated for each environment on all edge servers, requiring $O(N_{\mathrm{g}} E)$ operations per round. In each sampled environment, the number of operations required for the interaction processes is $O(T)$. Thus, for all environments in each round, these operations require $O(N_{\mathrm{g}} T)$ operations. For the neural network update section, as it involves operations such as replay of experiences and parameter modifications for Q functions and policy networks, the number of operations in each training round is $O(N_{\mathrm{up}} N_{\mathrm{net}})$. Therefore, in the $N_{\mathrm{ep}}$ training session, the computational complexity of this algorithm is $O(N_{\mathrm{ep}}(N_{\mathrm{g}}(E + T) + N_{\mathrm{up}} N_{\mathrm{net}}))$.

### D.2 Proof of Theorem 2

*Proof.* Since we aim to minimize the objective function Eq.10, and let $J(\pi) = \min_{\pi} \mathbb{E}\mathbf{x} \sim \pi \left[ \sum_{m \in \mathcal{M}} \gamma^m (\omega_{\mathrm{T}} T_m + \omega_{\mathrm{E}} E_m) \right]$, we hope $J(\pi_t) > J(\pi_{t+1})$. For any two adjacent policies $\pi_t$ and $\pi_{t+1}$, we derive a lower bound for their performance difference $\Delta J = J(\pi_t) - J(\pi_{t+1})$ as follows:

We first compute the performance difference for two adjacent policies:

$$\begin{aligned}\Delta J &= \left[\sum_{m\in\mathcal{M}} \gamma^m(\omega_T T_m(\pi_t) + \omega_E E_m(\pi_t))\right] \\ &\quad - \left[\sum_{m\in\mathcal{M}} \gamma^m(\omega_T T_m(\pi_{t+1}) + \omega_E E_m(\pi_{t+1}))\right] \\ &= \sum_{m\in\mathcal{M}} \gamma^m[\omega_T(T_m(\pi_t) - T_m(\pi_{t+1})) \\ &\quad + \omega_E(E_m(\pi_t) - E_m(\pi_{t+1}))]\end{aligned} \tag{A5}$$

The difference in energy consumption between the two policies is:

$$\begin{aligned}E_m(\pi_t) - E_m(\pi_{t+1}) &\geq p^{\text{off}} \sum_{e\in\mathcal{E}} [x_{m,e}(\pi_t) - x_{m,e}(\pi_{t+1})] \frac{L_m}{C_{u,e}} \\ &\quad + \sum_{e\in\mathcal{E}} [x_{m,e}(\pi_t) - x_{m,e}(\pi_{t+1})] \kappa\eta f_e^2 L_m\end{aligned} \tag{A6}$$

The difference in time consumption between the two policies is:

$$T_m(\pi_t) - T_m(\pi_{t+1}) \geq \hat{T}_m^{\text{off}}(\pi_t) - \hat{T}_m^{\text{off}}(\pi_{t+1}) \tag{A7}$$

Therefore, the lower bound for the performance difference between adjacent policies is:

$$\begin{aligned}\Delta J \geq \sum_{m\in\mathcal{M}} \gamma^m \{&\omega_E \sum_{e\in\mathcal{E}} [x_{m,e}(\pi_t) - x_{m,e}(\pi_{t+1})](p^{\text{off}} \frac{L_m}{C_{u,e}} \\ &+ \kappa\eta f_e^2 L_m) + \omega_T[\hat{T}_m^{\text{off}}(\pi_t) - \hat{T}_m^{\text{off}}(\pi_{t+1})]\}\end{aligned} \tag{A8}$$

Let $\Phi_{m,e} = p^{\text{off}} \frac{L_m}{C_{u,e}} + \kappa\eta f_e^2 L_m$ and $\Phi_{min} = \min_{m,e}\{\gamma^m \omega_E \Phi_{m,e}\}$
Then:

$$\Delta J \geq A\|\pi_t - \pi_{t+1}\|_1 \tag{A9}$$

where $A = \min\{\Phi_{min}, \min_m\{\gamma^m\omega_T\}\}$ and $\|\pi_t - \pi_{t+1}\|_1$ represents the L1-norm difference between the two policies.

## References


[1] G. Cui, X. Li, L. Xu, and W. Wang, "Latency and energy optimization for mec enhanced sat-iot networks," *IEEE Access*, vol. 8, pp. 55 915–55 926, 2020.

[2] L. Lei, H. Xu, X. Xiong, K. Zheng, W. Xiang, and X. Wang, "Multiuser resource control with deep reinforcement learning in iot edge computing," *IEEE Internet of Things J.*, vol. 6, no. 6, pp. 10 119–10 133, 2019.

[3] J. Li, H. Gao, T. Lv, and Y. Lu, "Deep reinforcement learning based computation offloading and resource allocation for mec," in *2018 IEEE Wireless Communications and Networking Conference (WCNC)*. IEEE, 2018, pp. 1–6.

[4] L. Huang, S. Bi, and Y.-J. A. Zhang, "Deep reinforcement learning for online computation offloading in wireless powered mobile-edge computing networks," *IEEE Transactions on Mobile Computing*, vol. 19, no. 11, pp. 2581–2593, 2019.

[5] D. C. Nguyen, P. N. Pathirana, M. Ding, and A. Seneviratne, "Deep reinforcement learning for collaborative offloading in heterogeneous edge networks," in *2021 IEEE/ACM 21st International Symposium on Cluster, Cloud and Internet Computing (CCGrid)*. IEEE, 2021, pp. 297–303.

[6] F. Jiang, L. Dong, K. Wang, K. Yang, and C. Pan, "Distributed resource scheduling for large-scale mec systems: A multiagent ensemble deep reinforcement learning with imitation acceleration," *IEEE Internet of Things Journal*, vol. 9, no. 9, pp. 6597–6610, 2021.

[7] Y. Li, J. Li, Z. Lv, H. Li, Y. Wang, and Z. Xu, "Gasto: A fast adaptive graph learning framework for edge computing empowered task offloading," *IEEE Transactions on Network and Service Management*, 2023.

[8] T. Ren, J. Niu, and Y. Qiu, "Enhancing generalization of computation offloading policies in novel mobile edge computing environments by exploiting experience utility," *Journal of Systems Architecture*, vol. 125, p. 102444, 2022.

[9] J. Wang, J. Hu, G. Min, A. Y. Zomaya, and N. Georgalas, "Fast adaptive task offloading in edge computing based on meta reinforcement learning," *IEEE Transactions on Parallel and Distributed Systems*, vol. 32, no. 1, pp. 242–253, 2020.

[10] T. Wu, W. Jing, X. Wen, Z. Lu, and S. Zhao, "A scalable computation offloading scheme for mec based on graph neural networks," in *2021 IEEE Globecom Workshops (GC Wkshps)*. IEEE, 2021, pp. 1–6.

[11] Z. Hu, J. Niu, T. Ren, and M. Guizani, "Achieving fast environment adaptation of drl-based computation offloading in mobile edge computing," *IEEE Transactions on Mobile Computing*, 2023.

[12] F. Jiang, K. Wang, L. Dong, C. Pan, and K. Yang, "Stacked autoencoder-based deep reinforcement learning for online resource scheduling in large-scale mec networks," *IEEE Internet of Things J.*, vol. 7, no. 10, pp. 9278–9290, 2020.

[13] N. Yang, J. Wen, M. Zhang, and M. Tang, "Multi-objective deep reinforcement learning for mobile edge computing," in *2023 21st international symposium on modeling and optimization in mobile, ad hoc, and wireless networks (WiOpt)*. IEEE, 2023, pp. 1–8.

[14] J. Chang, J. Wang, B. Li, Y. Zhao, and D. Li, "Attention-based deep reinforcement learning for edge user allocation," *IEEE Transactions on Network and Service Management*, 2023.

[15] Z. Gao, L. Yang, and Y. Dai, "Fast adaptive task offloading and resource allocation in large-scale mec systems via multi-agent graph reinforcement learning," *IEEE Internet of Things Journal*, 2023.

[16] L. Li, W. Chu, J. Langford, and R. E. Schapire, "A contextual-bandit approach to personalized news article recommendation," in *Proceedings of the 19th international conference on World wide web*, 2010, pp. 661–670.